Photoredox Catalysis

How to cite:
International Edition: doi.org/10.1002/anie.202107155
German Edition: doi.org/10.1002/ange.202107155

Red-Light-Mediated Photoredox Catalysis Enables Self-Reporting Nitric Oxide Release for Efficient Antibacterial Treatment

Zhiqiang Shen, Shaoqiu Zheng, Shiyan Xiao, Ruan Shen, Shiyong Liu,* and Jinming Hu**

Abstract: *Nitric oxide (NO) serves as a key regulator of many physiological processes and as a potent therapeutic agent. The local delivery of NO is important to achieve target therapeutic outcomes due to the toxicity of NO at high concentrations. Although light stimulus represents a non-invasive tool with spatiotemporal precision to mediate NO release, many photoresponsive NO-releasing molecules can only respond to ultraviolet (UV) or near-UV visible light with low penetration and high phototoxicity. We report that coumarin-based NO donors with maximal absorbances at 328 nm can be activated under (deep) red-light (630 or 700 nm) irradiation in the presence of palladium(II) tetraphenyltetrabenzoporphyrin, enabling stoichiometric and self-reporting NO release with a photolysis quantum yield of 8% via photoredox catalysis. This NO-releasing platform with ciprofloxacin loading can eradicate Pseudomonas aeruginosa biofilm in vitro and treat cutaneous abscesses in vivo.*

Introduction

Nitric oxide (NO), a diatom radical, has been recognized as the first gaseous signaling molecule, playing critical roles in many physiological and pathological processes.[1] The excellent contributions from Meyerhoff,[2] Handa,[3] Schoenfisch,[4] Reynolds,[5] and others[6] have revealed that NO could be used as a therapeutic agent as well, showing benefits in the treatment of cancers, bacterial infections, inflammatory diseases, and so on. Nevertheless, the systemic toxicity of NO at high concentrations necessitates local NO delivery to achieve target therapeutic outcomes.[7] To this end, NO-releasing molecules (NORMs) have been developed, including *N*-diazeniumdiolates, *S*-nitrosothiols, nitrate compounds, furoxans, metal nitrosyls, etc.[8] Notably, many NORMs suffered from spontaneous NO release, short half-lives, and (or) poor pharmacokinetics, impeding their biomedical applications. To circumvent this problem, the development of NORMs that can be selectively activated under specific stimuli has received increasing attention.[9] Of these, light irradiation represents a non-invasive means to regulate the NO release with advantages such as spatiotemporal control and tunable irradiation wavelengths/intensities.[10] However, conventional photoresponsive NORMs (photoNORMs) were primarily activated under ultraviolet (UV) or near-UV visible light, which was unfavorable for biomedical applications due to the inherent phototoxicity and limited tissue penetrations.[11]

To develop photoNORMs responsive to the phototherapeutic window (600–950 nm), two main approaches have been applied: (1) the introduction of chromophores with red or near-infrared (NIR)-absorbing capacity;[12] (2) the use of upconversion nanoparticles or two-photon absorption technique.[13] However, the former strategy generally led to decreased NO loading contents and water dispersity in biological fluids. The latter approach had to be operated at high excitation powers that typically surpassed the photodamage threshold of normal tissues.[14] To date, it remains a great challenge to develop photoNORMs with high NO loading contents that can release NO under the phototherapeutic window in biological fluids.

Herein, we report that the excited photosensitizers such as palladium(II) tetraphenyltetrabenzoporphyrin (PdTPTBP) derivatives can activate coumarin-based photoNORMs containing *N*-nitrosoamine moieties (CouN(NO)-R) under red-light irradiation (up to 700 nm), exhibiting self-reporting NO release with a remarkable fluorescence turn-on (Scheme 1 a). To demonstrate the potential biomedical applications, NO-releasing micelles were fabricated through the incorporation of PdTPTBP and CouN(NO)-R derivatives into micelle cores, showing red-light-triggered NO release in biological fluids and excellent antibiofilm activity in vitro. Moreover, the NO-releasing micelles could efficiently treat *Pseudomonas aeruginosa* (*P. aeruginosa*) infections in a cutaneous abscess model, synergistically eradicating bacterial pathogens and boosting wound healing.

Results and Discussion

Synthesis of coumarin-based NO donors. It is well-documented that *N*-nitrosoamine derivatives can release NO under light irradiation, and the excitation wavelengths could be switched by appending chromophores.[15] To date, both UV and visible light have been employed to activate *N*-nitrosoamine donors (Supporting Information, Figure S1). To facilitate the biomedical applications of these photoresponsive NO donors, the development of red or NIR light-responsive NO donors is of increasing interest due to increased tissue penetration and decreased phototoxicity.[12b]

[*] Z. Shen, S. Zheng, Prof. Dr. S. Xiao, R. Shen, Prof. Dr. S. Liu, Prof. Dr. J. Hu
CAS Key Laboratory of Soft Matter Chemistry
Hefei National Laboratory for Physical Science at the Microscale
Department of Polymer Science and Engineering
University of Science and Technology of China
Hefei 230026, Anhui (China)
E-mail: xiaosy@ustc.edu.cn
sliu@ustc.edu.cn
jmhu@ustc.edu.cn

Supporting information and the ORCID identification number(s) for the author(s) of this article can be found under: https://doi.org/10.1002/anie.202107155.

These are not the final page numbers!

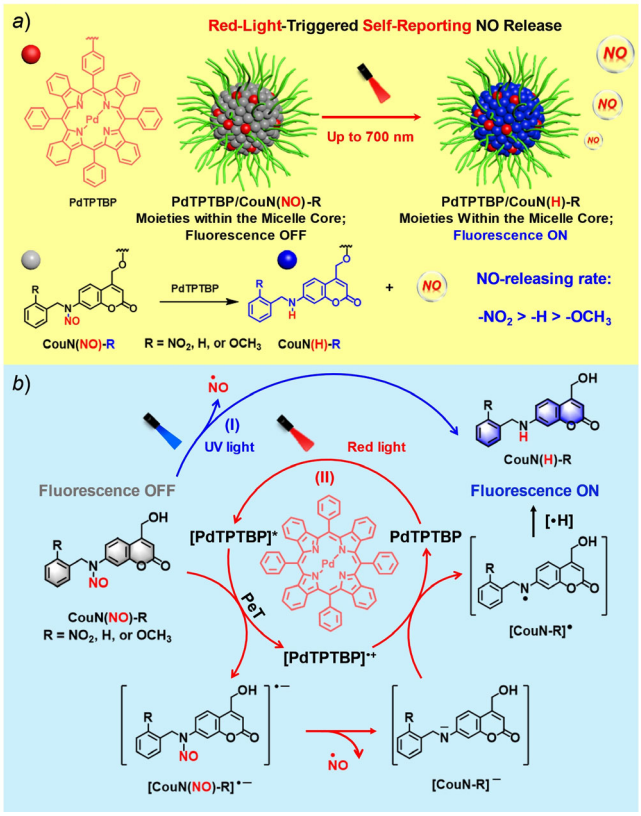

Scheme 1. a) Illustration of red-light-triggered self-reporting NO release from micellar nanoparticles containing both PdTPTBP photosensitizer and NO-releasing CouN(NO)-R moieties within the cores. b) Proposed mechanisms of the activation of CouN(NO)-R derivatives: (I) direct photolysis of CouN(NO)-R derivatives under UV light; (II) red-light-triggered NO release through photoredox catalysis.

However, the NO loading content, which was arbitrarily defined as the NO weight percentage in the NO donor, gradually decreased upon red-shifting the absorbance of the donors (Figure S1), which was unfavorable for biomedical applications.

In contrast to direct photolysis in the excited singlet state, triplet sensitization provided an indirect activation of latent acceptors through the triplet-triplet energy transfer (TTET) process.[16] We managed to activate *N*-nitrosoamine derivatives in the presence of suitable photosensitizers. To this end, we chose 7-aminocoumarin derivatives as the NO-releasing scaffold because of relatively high NO loading contents ($\approx$10 wt%) and the self-reporting NO release behavior.[17] Starting from 7-amino-4-hydroxymethyl-coumarin, three coumarin-based NO donors (CouN(NO)-R; R = NO_2, H, or OCH_3) were synthesized using similar protocols (Supporting Information, Scheme S1). The chemical structures of three NO donors were identified by ^1H and ^{13}C NMR spectroscopy and high-resolution mass spectrometry (HR-MS; Figures S2–S7).

Red-light-triggered NO release from CouN(NO)-R in the presence of PdTPTBP. CouN(NO)-NO_2 had maximal absorbance at 328 nm but no evident absorbance above 450 nm (Figure 1a). Under 365 nm light irradiation, photo-mediated NO release was achieved (Figure S8), confirming the photo-responsive nature of CouN(NO)-R derivatives. Upon screening specific photosensitizers, we unexpectedly found that a mixture of CouN(NO)-NO_2 (50 μM) and PdTPTBP (5 μM) showed a concurrent absorbance decrease at 328 nm and increase at 358 nm (Figure 1b), respectively, under mild red-light irradiation (630 nm, 30 mW cm^{-2}; this irradiation condition was used throughout this work). Note that the Soret and Q-bands of PdTPTBP were at 442 and 628 nm, respectively (Figure 1a). By sharp contrast, the control experiments revealed no absorbance changes without PdTPTBP, light irradiation, or CouN(NO)-NO_2 under otherwise identical conditions (Figure S9). Interestingly, we noticed that the absorbance spectra of CouN(NO)-NO_2 and PdTPTBP mixture after 630 nm light irradiation agreed quite well with the absorbance spectrum of CouN(H)-NO_2 (Figure S10a), implying the release of NO under 630 nm light irradiation. Electron paramagnetic resonance (EPR) spectra using 2-phenyl-4,4,5,5-tetramethyl-imidazoline-1-oxyl 3-oxide (PTIO) as the spin-trapping agent unequivocally revealed the release of NO radical (Figure 1c),[18] whereas no spontaneous NO release was observed without light irradiation or PdTPTBP, in line with the UV-vis results (Figure S9).

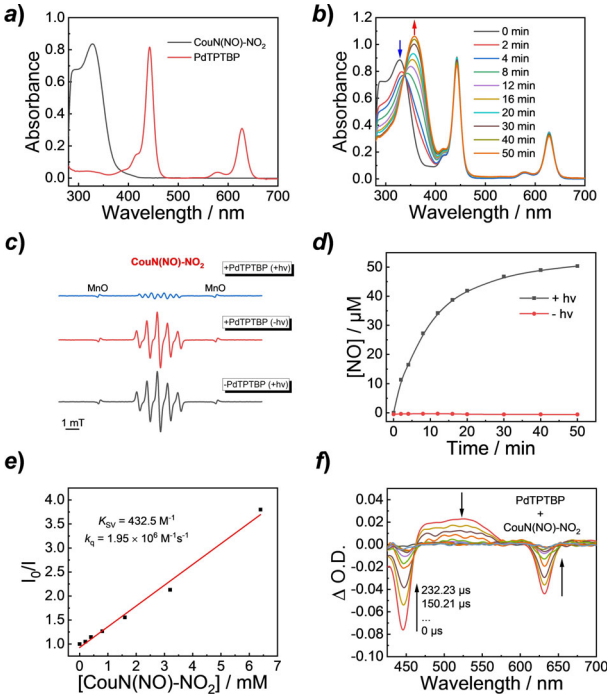

Figure 1. a) UV-vis absorbance spectra of PdTPTBP (5 μM) and CouN(NO)-NO_2 (50 μM) in DMSO. b) Evolution of UV-vis spectra of DMSO solution of CouN(NO)-NO_2 (50 μM) and PdTPTBP (5 μM) under 630 nm light irradiation (30 mW cm^{-2}). c) EPR spectra of CouN(NO)-NO_2 in the absence (black curve) and presence of PdTPTBP (5 μM) without (red curve) and with (blue curve) 630 nm light irradiation for 2 min. In all cases, the concentrations of PTIO and CouN(NO)-NO_2 were 20 and 50 μM, respectively. d) NO release profiles of DMSO solution of CouN(NO)-NO_2 (50 μM) and PdTPTBP (5 μM) mixture with or without 630 nm irradiation (30 mW cm^{-2}). e) Stern–Volmer plot of phosphorescence intensity quenching of PdTPTBP (10 μM) by CouN(NO)-NO_2 in Ar-saturated DMSO. f) Nanosecond time-resolved transient absorption spectra (λ_{ex} = 630 nm) of PdTPTBP (10 μM) and CouN(NO)-NO_2 (10 mM) in Ar-saturated DMSO.

It is challenging to monitor the NO release in real-time due to the high reactivity of NO,[19] while the NO release contents could be calculated by the absorbance changes due to the quantitative conversion of CouN(NO)-NO_2 to CouN-(H)-NO_2 (Figure S11). We found that the NO release amounts reached a plateau after ≈50 min light irradiation (Figure 1d), releasing NO in a stoichiometric manner with a photolysis quantum yield of 8% (see Supporting Information for details). Notably, both the NO-releasing amounts and rates under 630 nm light irradiation were higher than that of 365 nm light irradiation, which was likely due to the side reactions under UV light irradiation (Figure S8). Moreover, the NO release profiles can be tuned by changing the PdTPTBP concentrations, and an increased PdTPTBP concentration led to a faster NO-releasing rate (Supporting Information, Figure S12, Table S1). Since CouN(NO)-NO_2 itself cannot release NO under 630 nm light irradiation, it was assumed that the red-light-triggered NO release was ascribed to the indirect activation of CouN(NO)-NO_2 in the presence of PdTPTBP. To confirm this assumption, we investigated the photoluminescence of PdTPTBP with varying amounts of CouN(NO)-NO_2. Both the phosphoresce intensities and lifetimes of PdTPTBP were drastically quenched upon increasing the concentrations of CouN-(NO)-NO_2 donor (Figures 1e; Figure S13), demonstrating that the excited PdTPTBP can be quenched by CouN(NO)-NO_2 through either an energy or electron transfer process. Specifically, the Stern–Volmer constant (K_{SV}) and the quenching rate constant (k_q) was calculated to be 432.5 M^{-1} and 1.95×10^6 $M^{-1}s^{-1}$ (Figure 1e). This quenching process was further corroborated by nanosecond transient absorption spectra (Figure 1f; Figure S14).

Having confirmed that it was possible to regulate the NO release from CouN(NO)-NO_2 by red-light irradiation, we next sought to test whether CouN(NO)-H and CouN(NO)-OCH_3 could be activated under the same conditions. Although there were no absorbance changes without 630 nm light irradiation, similar changes in UV-vis spectra were observed for both CouN(NO)-H and CouN(NO)-OCH_3 under 630 nm irradiation (Figure S15). Quantitative analysis by comparing the absorption ratio changes (A_{358nm}/A_{328nm}) revealed that the NO-releasing rates were in the order of CouN(NO)-NO_2 > CouN(NO)-H > CouN(NO)-OCH_3 (Figure S16, Table S2), revealing that the electronic effect played a critical role on the NO-releasing rates. In addition to varying NO donors, we also examined the NO-releasing behavior in the presence of distinct photosensitizers. Using CouN(NO)-NO_2 as an example, the photo-mediated NO release could also be established in the presence of 5,10,15,20-(tetraphenyl)tetrabenzoporphyrin (H_2TPTBP). Albeit slower, the use of metal-free H_2TPTBP rendered it possible to achieve the NO release under 700 nm light irradiation (Figures S17 and S18, Table S3), which was rather appealing for biomedical applications due to the further increased tissue penetration and decreased phototoxicity.

Red-light-triggered NO release from micellar nanoparticles. After confirming red-light-triggered NO release in organic solvents (i.e., DMSO), we attempted to investigate whether the red-light-activatable NO-releasing platform could be operated in purely aqueous media. Notably, many previous triplet sensitization systems can only be operated in organic solvents or solid states and suffered from partial or complete loss of efficiency in aqueous solutions.[20] Due to the poor water-solubility of CouN(NO)-R and PdTPTBP derivatives, we covalently incorporated both the NO-releasing moieties and PdTPTBP into the cores of micellar nanoparticles. To this end, the hydroxyl groups of CouN(NO)-NO_2 and CouN(H)-NO_2 were functionalized with 2-isocyanatoethyl methacrylate with the formation of CouN(NO) and CouN(H) monomers, respectively (Scheme S2a). In addition, the PdTPTBP monomer was also synthesized (Scheme S2b). The chemical structures of all monomers were characterized by the combination of NMR, HR-MS, and high-performance liquid chromatography (HPLC; Figures S19–S22). Interestingly, the formation of CouN(NO) monomer did not compromise the NO release capacity, and the conversion of CouN(NO) to CouN(H) with the release of NO in the presence of PdTPTBP was confirmed by HR-MS analysis (Figure S23). Although the carbamate linkage in the 4-position of coumarin derivatives can also be photo-activated,[21] only the *N*-nitrosoamine moieties were selectively activated under the current circumstances (Figure S23). In order to fabricate NO-releasing micelles, we used reversible addition-fragmentation chain transfer (RAFT) polymerization to copolymerize PdTPTBP and CouN(NO) monomers by taking advantage of the versatility in monomer compatibility of RAFT polymerization. Besides conventional poly(ethylene glycol)(PEG)-based macroRAFT agent, we also prepared PGal homopolymer through the RAFT polymerization of galactose-based monomer (Gal), which was known to specifically bind to Lectin A (LecA) in *P. aeruginosa* (Scheme S2c, Figures S24 and S25).[22] With the macroRAFT agents and monomers in hand, amphiphilic block copolymers (PGalNP, PGalHP, PEGNP, and PGalN) were then synthesized (Scheme 2; Scheme S3) and characterized (Figures S26–S29, Table S4).

All the block copolymers self-assembled into micellar nanoparticles in aqueous solutions with diameters of 50–70 nm, and the exposure to 630 nm light irradiation did not significantly affect the micellar sizes (Figure 2a,b; Figure S30). Moreover, all micellar nanoparticles had negative zeta potentials of −8 to −12 mV, showing negligible changes under irradiation (Figure S31). However, we observed concurrent absorbance decreases at 328 nm and increases at 358 nm of PGalNP micelles in the presence of sodium ascorbate (Figure 2c). The changes of UV-vis spectra were similar to that of the CouN(NO)-NO_2 precursor in the presence of PdTPTBP in DMSO (Figure 1b), indicating photo-triggered NO release under 630 nm light irradiation. Moreover, the NO-releasing profiles can be tuned by irradiation intensities, and a higher irradiation intensity led to a fast NO release (Figure S32). By sharp contrast, there was no appreciable NO release without 630 nm light irradiation or sodium ascorbate (Figure S33). Notably, the triple-state of photosensitizers was readily quenched by oxygen, and sodium ascorbate was used to scavenge the produced singlet oxygen (Figure S34).[23] Moreover, we found that PEGNP micelles with the same core but different coronas showed similar

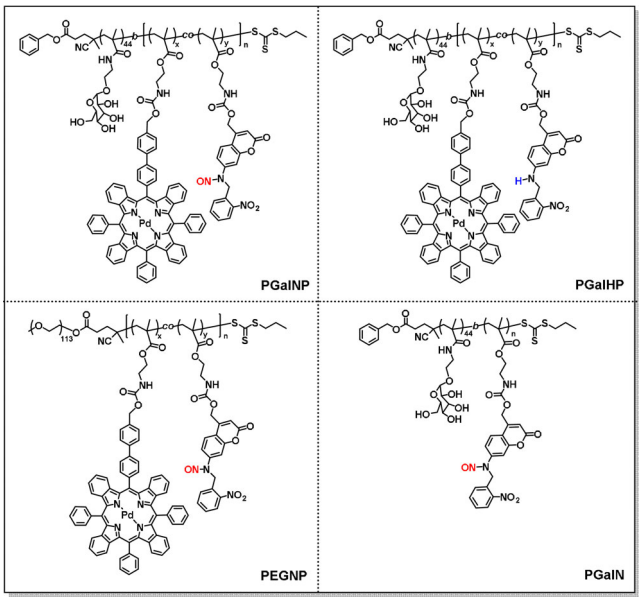

Scheme 2. Chemical structures of PGalNP, PGalHP, PEGNP, and PGalN diblock copolymers.

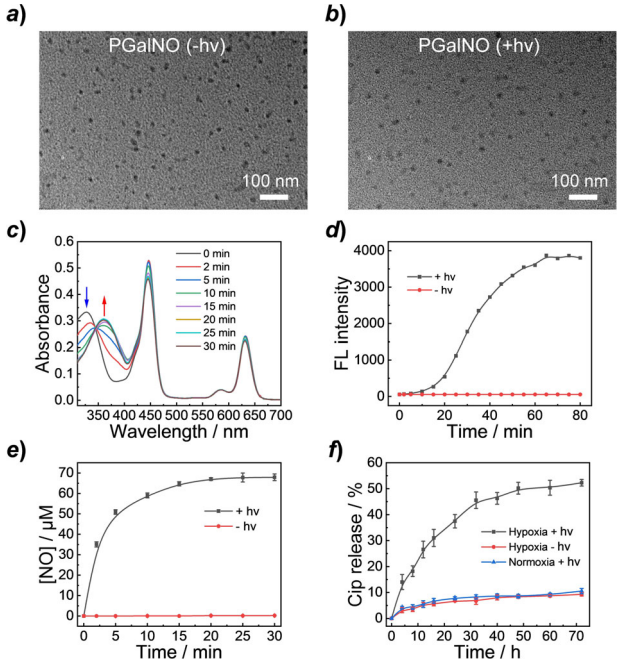

Figure 2. TEM images of PGalNP micelles a) before and b) after 630 nm irradiation for 30 min. Evolution of c) UV-vis spectra PGalNP micelles (0.1 $g\,L^{-1}$) in the presence of sodium ascorbate (10 mM) under 630 nm irradiation. d) Fluorescence intensity changes of PGalNP micelles (0.1 $g\,L^{-1}$) in the presence of sodium ascorbate (10 mM) under 630 nm irradiation. e) NO release profiles and f) Ciprofloxacin (Cip) release profiles from Cip@PGalNP micelles under varying conditions. Data are shown as mean ± s.d. ($n=3$). In all cases, the irradiation intensity was 30 $mW\,cm^{-2}$.

NO-releasing performance (Figure S35), revealing that the NO release process was not affected by the hydrophilic corona. However, for PGalN micelles without the labeling of PdTPTBP, no changes in UV-vis spectra were observed, regardless of with or without 630 nm light irradiation (Figure S36). These results not only precluded spontaneous NO release but also demonstrated the critical role of PdTPTBP for red-light-mediated NO release.

The NO release with the generation of CouN(H)-NO_2 moieties within micellar cores led to the fluorescence turn-on, exhibiting ≈70-fold fluorescence increase (Figure 2d; Figure S37). The released NO content was calculated to be ≈70 μM at a PGalNP micelle concentration of 0.1 $g\,L^{-1}$ under 630 nm irradiation for 20 min (Figure 2e), corresponding to ≈78% of CouN(NO)-NO_2 moieties within the micelle cores. Moreover, although the NO release did not lead to the micellar disassembly, we found that the encapsulated payload such as ciprofloxacin (Cip) was released under 630 nm light irradiation, enabling the corelease of NO and Cip (Figure 2f; Figure S38).

Red-light-triggered NO release for *P. aeruginosa* biofilm dispersal. Considering the red-light-triggered NO release from PGalNP micelles in aqueous solutions, subsequently, we investigated the antibiofilm performance by using the local NO release.[24] *P. aeruginosa* has been known as an opportunistic microbe, accounting for 10–20% of nosocomial infections. Even worse, the formation of *P. aeruginosa* biofilm renders it more resistant to conventional antibiotics and more difficult to treat.[22] In vitro antibiofilm experiments revealed that although Cip (10 $\mu g\,mL^{-1}$, identical to the Cip concentration in Cip@PGalNP micelles of 0.2 $g\,L^{-1}$) cannot efficiently eradicate the biofilm, NO-releasing micelles of PEGNP, PGalNP, and Cip-loaded PGalNP (Cip@PGalNP) led to 37.1%, 70.9%, and 96.7% decrease in the biofilm biomass after 630 nm light irradiation for 30 min, as determined by the crystal violet staining (Figure 3a; Figure S39). The bacterial viability was further analyzed by colony-forming unit (CFU) assay, revealing that Cip@PGalNP displayed the best antibiofilm performance as well (Figure 3b).

To ascertain the cause of biofilm dispersal, we quantified the nitrite concentrations within the biofilms by Griess assay,[25] revealing the increased nitrite concentrations of PEGNP, PGalNP, and Cip@PGalNP micelles after 630 nm light irradiation (Figure 3c; Figure S40). This result suggested that the red-light-triggered NO release from the micellar nanoparticles resulted in biofilm dispersal. Interestingly, PGalNP exhibited better antibiofilm performance than that of PEGNP with similar NO loading contents yet different coronas. The increased antibiofilm capacity was likely due to the presence of galactose moieties, facilitating the penetration of PGalNP micelles within the biofilm via binding to the LecA of bacteria.[22] The increased biofilm penetration was important to boost the NO release because of the increased hypoxic condition within the interior of biofilms.[26] Indeed, the increased NO release of PGalNP micelles was observed (Figure 3c).

Moreover, we used confocal laser scanning microscopy (CLSM) to directly observe the NO-mediated biofilm dispersal (Scheme S4). Despite no evident biofilm dispersal subjected to 630 nm light irradiation or Cip addition, we observed decreased *P. aeruginosa* biofilms for PEGNP, PGalNP, and Cip@PGalNP micelles under 630 nm light

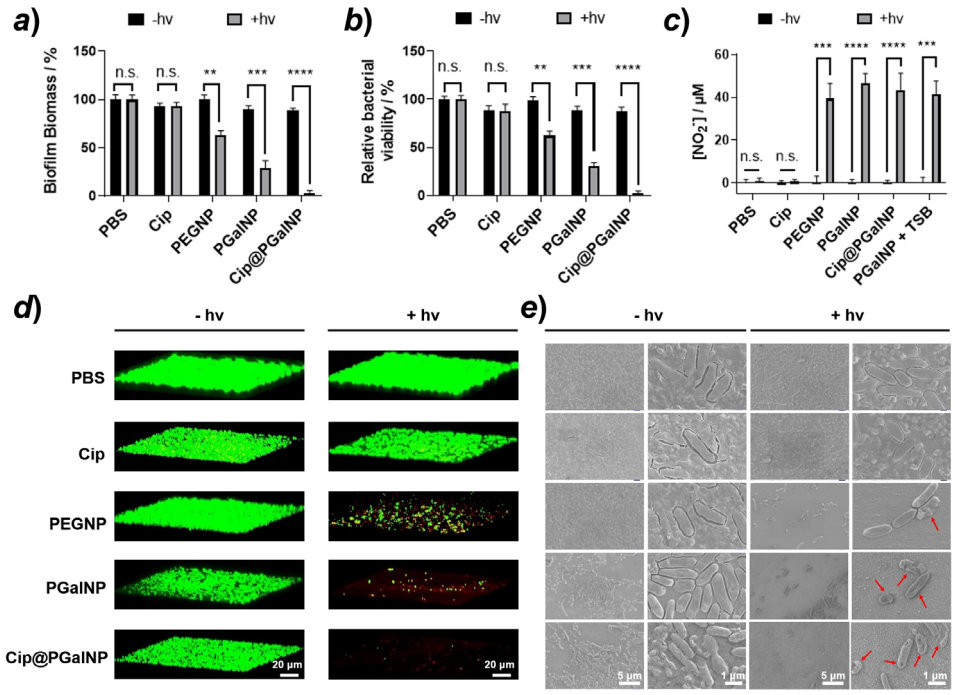

Figure 3. a) Bacterial biomass of *P. aeruginosa* biofilms by crystal violet staining and b) corresponding bacterial viability after treatment with free Cip and PEGNP, PGalNP, and Cip@PGalNP micelles without or with 630 nm light irradiation for 30 min, respectively. c) Quantification of nitrite concentrations by Griess assay after treatment with free Cip and PEGNP, PGalNP, and Cip@PGalNP micelles without or with 630 nm light irradiation for 30 min, respectively. Data are shown as mean ± s.d. ($n=3$); p values were calculated in comparison with the non-irradiated groups. $^{**}p<0.01$; $^{***}p<0.001$; $^{****}p<0.0001$; n.s., not significant. d) 3D CLSM images of *P. aeruginosa* biofilms stained with the LIVE/DEAD® BacLight bacterial viability kit, which were treated with free Cip and PEGNP, PGalNP, and Cip@PGalNP micelles without or with 630 nm light irradiation for 30 min (30 mW cm^{-2}), respectively. The green and red channels were excited with a 488 nm laser and were collected at 500–545 nm (green) and 600–650 nm (red), respectively. e) SEM images of *P. aeruginosa* biofilms treated with free Cip or PEGNP, PGalNP, and Cip@PGalNP micelles without or with 630 nm light irradiation for 30 min (30 mW cm^{-2}), respectively. The arrows indicate dead bacteria with disrupted membrane integrity. In all cases, the Cip and micelle concentrations were 10 μg mL^{-1} and 0.2 g L^{-1}, respectively.

irradiation (Figure S41). Notably, the NO-mediated biofilm dispersal was accompanied by the appearance of blue fluorescence due to the in situ conversion of non-fluorescent CouN(NO)-NO_2 to fluorescent CouN(H)-NO_2 moieties (Figure S37). More importantly, the red-light-triggered NO release not only efficiently eradicated the biofilm but also killed bacterial pathogens, as indicated by the LIVE/DEAD® BacLight bacterial viability kit staining (Figure 3d). Cip@PGalNP micelles showed the best antibiofilm performance, as evidenced by the significantly decreased green fluorescence (living bacteria) and increased yellow and red fluorescence (dead bacteria). Moreover, NO-mediated biofilm dispersal was also confirmed by scanning electron microscopy (SEM) analysis, revealing the efficient biofilm eradication and disruption of bacterial membrane integrity under 630 nm light irradiation (Figure 3e).[27]

Treatment of *P. aeruginosa* infection in a cutaneous abscess model. After in vitro screening of the antibiofilm and antibacterial performance of NO-releasing micelles, we chose PGalNP micelles with better antibacterial activity to further explore the anti-infection applications in vivo. Cutaneous abscess infections are very common and difficult to treat with conventional antibiotics, and it is highly desirable to develop new therapeutic agents for efficient abscess treatment.[28] NO-releasing nanoparticles have previously been used for the treatment of bacterial infections with the advantages of no drug-resistance development and accelerated wound healing.[29] We subcutaneously injected *P. aeruginosa* PAO1 microbes into mice to develop skin abscesses.[26a] The bacterial proliferation could be in-vivo-monitored by the GFP fluorescence of PAO1 (Figure S42). After 48 h of infection, cutaneous abscesses with evident dermonecrosis and white lesions (filled with fluid/pus) were formed. The infected mice were randomly divided into five groups, receiving different treatments including PBS, Cip, PGalNP micelles with 630 nm light irradiation, Cip@PGalNP micelles without and with 630 nm light irradiation, respectively. At predetermined times, the abscesses were imaged, the bacterial burden in the lesion tissues was counted, and the lesion tissues were evaluated by histological analysis (Figure 4a).

The infected mice receiving PBS and Cip treatments showed negligible changes in the abscess areas throughout the therapeutic procedure. However, PGalNP micelles with 630 nm light irradiation efficiently accelerated the lesion healing, and the corelease of Cip and NO from Cip@PGalNP micelles further augmented the therapeutic outcomes (Figure 4b,c). By striking contrast, Cip@PGalNP micelles without 630 nm irradiation did not show evident therapeutic benefits compared with the PBS control, indicating that the red-light-triggered corelease of NO and Cip played a critical role in the antibacterial effect. To prove the NO release in vivo under 630 nm light irradiation, we used a NO-specific fluorescence probe (i.e., RhBP, Figure S43) to detect the NO release.[30] The formation of highly emissive rhodamine B was observed for PGalNP micelle in the presence of RhBP probe with 630 nm light irradiation, whereas control experiments using either PGalNP micelles with RhBP without irradiation, PGalHP micelles without NO-releasing capacity with or without 630 nm light irradiation, or PGalNP micelles without RhBP probe with or without 630 nm light irradiation revealed no detectable emission of RhB (Figure S43). This result potently revealed that red-light-triggered NO release from PGalNP micelles

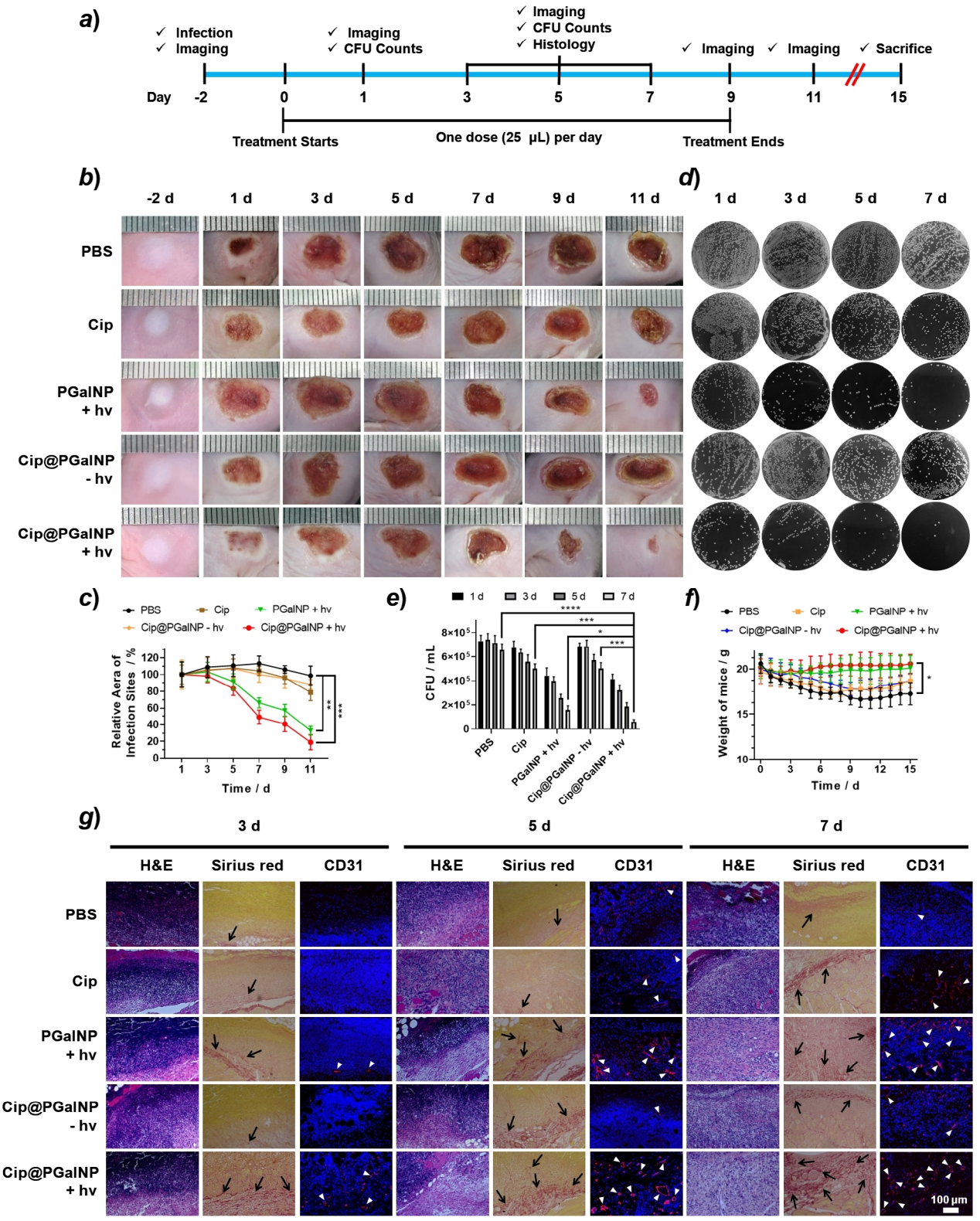

Figure 4. a) Experimental timeline of in vivo treatment of bacterial infection in a cutaneous abscess model. b) Representative images of the abscess during the treatment process and c) quantitative analysis of the infected areas receiving different treatments. $^{**}p<0.01$, $^{***}p<0.001$ compared with the PBS group. d) Photographs of bacterial colonies on the agar plates of the abscess tissues with varying treatments. e) Bacterial colony-forming unit separated from abscess tissues with varying treatments. $^{*}p<0.05$, $^{***}p<0.001$, $^{****}p<0.0001$, compared with the group receiving Cip@PGaINP (+hv) treatment on day 7. f) Changes of body weights of *P. aeruginosa* biofilm-infected mice after different treatments. $^{*}p<0.05$. g) Histological and immunofluorescence analysis on days 3, 5, and 7 of the mice infected with *P. aeruginosa* receiving varying treatments (the black arrows indicate collagen deposition and white triangles suggest re-epithelialization). Scale bar: 100 μm. In all cases, the Cip and micelle concentrations were 10 $\mu g\,mL^{-1}$ and 0.2 $g\,L^{-1}$, respectively.

could be in situ detected by RhBP probe. Therefore, the red-light-triggered NO release can be achieved in physiological conditions, representing a feasible approach to locally deliver NO.

Quantitative analysis by CFU assay of the abscess tissues after various treatments revealed that the least bacterial burden of Cip@PGalNP-treated group under 630 nm light irradiation (Figure 4d,e). Moreover, the Cip@PGalNP-treated group resulted in the recovery of body weights (Figure 4f). Histological and immunofluorescence analyses revealed that the red-light-mediated NO release from Cip@PGalNP micelles markedly decreased the infiltration of inflammatory cells, boosted collagen deposition in the wound areas, and facilitated re-epithelialization, in line with the physiological effects of NO in accelerating lesion healing (Figure 4g).[31] Importantly, we found that PGalNP micelles exhibited negligible toxicity toward normal mammalian cells such as L929 cells (Figure S44). In addition, PGalNP and PGalHP micelles showed negligible hemolysis behavior (Figure S45). Hence, the NO-releasing PGalNP could be potentially used as a novel antibiofilm and antibacterial agent with low toxicity toward normal cells.

Study on NO-releasing mechanism. PdTPTBP photosensitizer was overwhelmingly used as a triplet energy donor in triplet-triplet annihilation upconversion (TTA-UC) due to the relatively high triplet energy level.[21b,23,32] We first hypothesized that the activation of CouN(NO)-R moieties in the presence of PdTPTBP through a TTET process. As such, we calculated the triplet energy of PdTPTBP and CouN(NO)-R moieties. The triplet energy (T_1) of the PdTPTBP monomer was determined to be ≈1.55 eV according to the phosphorescence emission spectrum (Figure S46). The T_1 energy of CouN(NO)-NO_2, CouN(NO)-H, and CouN(NO)-OCH_3 were calculated to be 2.15, 2.17, and 2.23 eV, respectively, using time-dependent density functional theory (TDDFT) at the level of B3LYP/6–31+G(d, p), which were much higher than that of PdTPTBP (>0.6 eV), precluding the possibility of activation of CouN(NO)-R moieties through a TTET mechanism.[16a] However, we found that the PdTPTBP monomer had a LUMO energy level of −2.61 eV, which was higher than CouN(NO)-NO_2 (−3.14 eV). This higher LUMO energy level provided a driving force for the electron transfer (ET) from PdTPTBP to CouN(NO)-NO_2 upon excitation. By contrast, the LUMO energy levels of CouN(NO)-H (−2.57 eV) and CouN(NO)-OCH_3 (−2.44 eV) were higher than that of PdTPTBP, indicating unfavorable ET from PdTPTBP (Figure 5a). The above result led to the postulation that the NO release from CouN(NO)-R was activated through a photoinduced electron transfer (PeT) process.

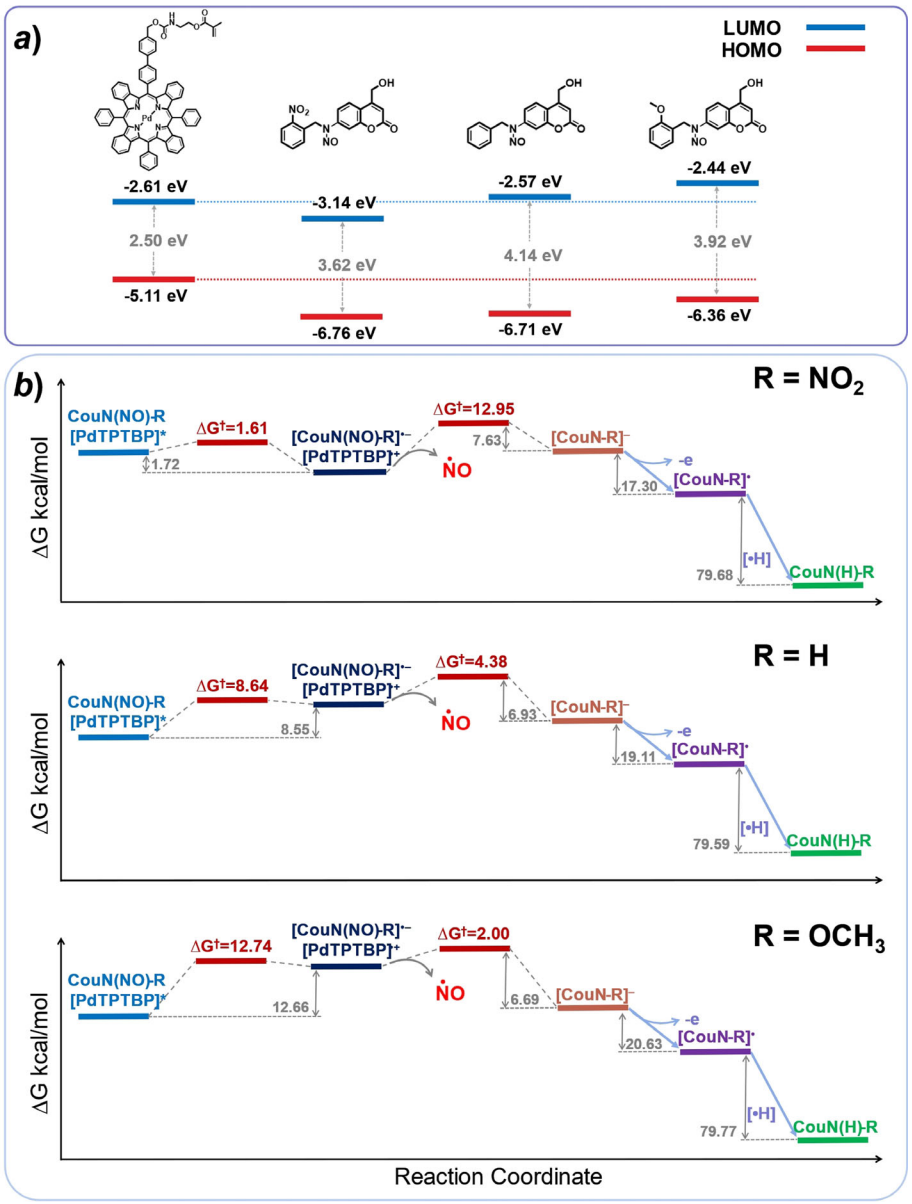

Figure 5. a) The relative energetic dispositions for the frontier orbitals (HOMO and LUMO) of PdTPTBP monomer and CouN(NO)-R derivatives. b) Free energy profiles for the PeT process from the triple excited state of [PdTPTBP]* ([D]*) to CouN(NO)-R (A(NO)) under red-light irradiation: red-light-mediated electron transfer ($[D]^* + A(NO) \rightarrow [D]^{\cdot+} + [A(NO)]^{\cdot-}$), the subsequent NO release ($[A(NO)]^{\cdot-} \rightarrow [A]^- + {}^{\cdot}NO$), the conversion of $[A]^-$ to $[A]^{\cdot}$ through the ET from $[A]^-$ to $[D]^{\cdot+}$, and the combination of $[A]^{\cdot}$ and $[{}^{\cdot}H]$ into AH. DFT calculations were performed at the B3LYP/6-31+G(d,p) level.

To confirm the PeT mechanism, we measured the excited redox potential of $E_{1/2}$(PdTBTBP$^{\bullet+}$/PdTPTBP*) using cyclic voltammetry, which was determined to be −0.8 V (potential vs. an Ag/AgCl electrode in DMF). The reduction potentials of CouN(NO)-NO_2, CouN(NO)-H, and CouN(NO)-OCH_3 were calculated to be −0.74, −1.17, and −1.21 V, respectively (Figure S47). As such, PdTBTBP could potentially reduce CouN(NO)-NO_2 at the excited state, whereas the reduction of CouN(NO)-H and CouN(NO)-OCH_3 was less effective, in good agreement with the decreased NO-releasing rates (Table S2). Moreover, we applied the Marcus theory[33] to calculate the activation Gibbs free energy barrier of the ET from [PdTPTBP]* to CouN(NO)-R moieties (Figure S48). Remarkably, the energy barrier for the ET reaction between [PdTPTBP]* and CouN(NO)-NO_2 was as low as $\Delta G^{\dagger} = 1.61\ \text{kcal mol}^{-1}$, whereas much higher barriers were observed for CouN(NO)-H and CouN(NO)-OCH_3 (8.64 and 12.74 kcal mol^{-1}; Figure 5b).

Building on the above results, we proposed the following mechanism for NO release. Upon red-light excitation, the excited PdTPTBP in its triplet state reduced CouN(NO)-R moieties via ET with the formation of [CouN(NO)-R]$^{\bullet-}$. Then, [CouN(NO)-R]$^{\bullet-}$ species underwent spontaneously release of NO radical with the formation of [CouN-R]$^{-}$, while [CouN-R]$^{-}$ was oxidized to [CouN-R]$^{\bullet}$ after the reduction of [PdTPTBP]$^{\bullet+}$ to PdTPTBP, and the [CouN-R]$^{\bullet}$ intermediate was further transformed to CouN(H)-R following abstraction of [$^{\bullet}$H] with fluorescence turn-on, enabling red-light-mediated NO release through photoredox catalysis (Scheme 1b). Although PdTPTBP was primarily used as a triplet donor rather than a photoredox catalyst,[23,32a,b] our results, for the first time, revealed that PdTPTBP photosensitizer could be used as a photoredox catalyst as well, which may broaden the potential applications of PdTPTBP derivatives in terms of photoredox catalysis,[34] polymerizations,[35] etc.

Conclusion

In summary, we have successfully achieved local delivery of NO under (deep) red-light irradiation through photoredox catalysis between PdTPTBP and CouN(NO)-R derivatives. We showed that the NO release process was not affected in biological fluids by incorporating both PdTPTBP and NO-releasing monomers into micelle cores. The resultant NO-releasing micelles cannot only disperse *P. aeruginosa* biofilms but also eradicate bacterial pathogens in vitro. Further, we confirmed that the NO-releasing micelles with low cytotoxicity to normal mammalian cells could efficiently treat bacterial infection in a cutaneous abscess model, exhibiting excellent antibacterial performance and accelerating wound healing. This work sheds light on local delivery of NO by taking advantage of (deep) red light, paving the way toward new photoresponsive NO-releasing materials for biomedical applications.

Acknowledgements

The authors gratefully acknowledge the financial support of the National Key R&D Program of China (2020YFA0710700), the National Natural Scientific Foundation of China (NNSFC) Projects (51690150, 51690154, 52073270, 51722307, and 22073090), and the Fundamental Research Funds for the Central Universities (WK2060190102).

Conflict of Interest

The authors declare no conflict of interest.

Keywords: abscess · antibiofilm · bacterial infection · nitric oxide · self-reporting release

[1] a) C. Farah, L. Y. M. Michel, J. L. Balligand, *Nat. Rev. Cardiol.* **2018**, *15*, 292–316; b) K. M. Dillon, R. J. Carrazzone, J. B. Matson, K. Kashfi, *Biochem. Pharmacol.* **2020**, *176*, 113931.
[2] a) Y. Q. Wo, E. J. Brisbois, R. H. Bartlett, M. E. Meyerhoff, *Biomater. Sci.* **2016**, *4*, 1161–1183; b) W. Y. Cai, J. F. Wu, C. W. Xi, M. E. Meyerhoff, *Biomaterials* **2012**, *33*, 7933–7944.
[3] a) P. Singha, J. Locklin, H. Handa, *Acta Biomater.* **2017**, *50*, 20–40; b) J. Pant, M. J. Goudie, S. P. Hopkins, E. J. Brisbois, H. Handa, *ACS Appl. Mater. Interfaces* **2017**, *9*, 15254–15264.
[4] a) L. Yang, E. S. Feura, M. J. R. Ahonen, M. H. Schoenfisch, *Adv. Healthcare Mater.* **2018**, *7*, 1800155; b) H. B. Jin, L. Yang, M. J. R. Ahonen, M. H. Schoenfisch, *J. Am. Chem. Soc.* **2018**, *140*, 14178–14184.
[5] a) A. Pegalajar-Jurado, K. A. Wold, J. M. Joslin, B. H. Neufeld, K. A. Arabea, L. A. Suazo, S. L. McDaniel, R. A. Bowen, M. M. Reynolds, *J. Controlled Release* **2015**, *217*, 228–234; b) J. L. Gordon, K. J. Hinsen, M. M. Reynolds, T. A. Smith, H. O. Tucker, M. A. Brown, *RSC Adv.* **2021**, *11*, 9112–9120.
[6] a) S. Y. Tao, J. Cheng, G. Su, D. Li, Z. Q. Shen, F. H. Tao, T. You, J. M. Hu, *Angew. Chem. Int. Ed.* **2020**, *59*, 21864–21869; *Angew. Chem.* **2020**, *132*, 22048–22053; b) M. C. Jen, M. C. Serrano, R. van Lith, G. A. Ameer, *Adv. Funct. Mater.* **2012**, *22*, 239–260; c) G. R. Jin, Z. Y. Gao, Y. J. Liu, J. Zhao, H. L. Ou, F. Xu, D. Ding, *Adv. Healthcare Mater.* **2021**, *10*, 2001550.
[7] a) S. P. Nichols, W. L. Storm, A. Koh, M. H. Schoenfisch, *Adv. Drug Delivery Rev.* **2012**, *64*, 1177–1188; b) K. Sharma, H. Chakrapani, *Nitric Oxide* **2014**, *43*, 8–16.
[8] a) Y. Q. Yang, Z. J. Huang, L. L. Li, *Nanoscale* **2021**, *13*, 444–459; b) P. G. Wang, M. Xian, X. P. Tang, X. J. Wu, Z. Wen, T. W. Cai, A. J. Janczuk, *Chem. Rev.* **2002**, *102*, 1091–1134.
[9] a) T. Yang, A. N. Zelikin, R. Chandrawati, *Small* **2020**, *16*, 1907635; b) W. P. Fan, B. C. Yung, X. Y. Chen, *Angew. Chem. Int. Ed.* **2018**, *57*, 8383–8394; *Angew. Chem.* **2018**, *130*, 8516–8528.
[10] a) H. Nakagawa, *Nitric Oxide* **2011**, *25*, 195–200; b) T. Bian, Z. L. Chu, R. Klajn, *Adv. Mater.* **2020**, *32*, 1905866.
[11] S. Sortino, *Chem. Soc. Rev.* **2010**, *39*, 2903–2913.
[12] a) N. Ieda, Y. Hotta, A. Yamauchi, A. Nishikawa, T. Sasamori, D. Saitoh, M. Kawaguchi, K. Kimura, H. Nakagawa, *ACS Chem. Biol.* **2020**, *15*, 2958–2965; b) E. Y. Zhou, H. J. Knox, C. J. Reinhardt, G. Partipilo, M. J. Nilges, J. Chan, *J. Am. Chem. Soc.* **2018**, *140*, 11686–11697.
[13] a) Y. Q. Jiang, P. F. Fu, Y. Y. Liu, C. C. Wang, P. R. Zhao, X. Chu, X. W. Jiang, W. Yang, Y. L. Wu, Y. Wang, G. H. Xu, J. Hu, W. B. Bu, *Sci. Adv.* **2020**, *6*, eabc3513; b) X. Zhang, J. F. Du, Z. Guo, J. Yu, Q. Gao, W. Y. Yin, S. Zhu, Z. J. Gu, Y. L. Zhao, *Adv. Sci.* **2019**, *6*, 1801122.

[14] G. Y. Chen, H. L. Qju, P. N. Prasad, X. Y. Chen, *Chem. Rev.* **2014**, *114*, 5161 – 5214.
[15] a) C. Parisi, M. Failla, A. Fraix, B. Rolando, E. Gianquinto, F. Spyrakis, E. Gazzano, C. Riganti, L. Lazzarato, R. Fruttero, A. Gasco, S. Sortino, *Chem. Eur. J.* **2019**, *25*, 11080 – 11084; b) N. Ieda, Y. Hotta, N. Miyata, K. Kimura, H. Nakagawa, *J. Am. Chem. Soc.* **2014**, *136*, 7085 – 7091; c) S. Namiki, T. Arai, K. Fujimori, *J. Am. Chem. Soc.* **1997**, *119*, 3840 – 3841.
[16] a) W. Lv, Y. F. Li, F. Y. Li, X. Lan, Y. M. Zhang, L. L. Du, Q. Zhao, D. L. Phillips, W. P. Wang, *J. Am. Chem. Soc.* **2019**, *141*, 17482 – 17486; b) S. H. C. Askes, G. U. Reddy, R. Wyrwa, S. Bonnet, A. Schiller, *J. Am. Chem. Soc.* **2017**, *139*, 15292 – 15295.
[17] Z. Q. Shen, K. W. He, Z. L. Ding, M. D. Zhang, Y. Q. Yu, J. M. Hu, *Macromolecules* **2019**, *52*, 7668 – 7677.
[18] Y. T. Duan, Y. Wang, X. H. Li, G. Z. Zhang, G. Y. Zhang, J. M. Hu, *Chem. Sci.* **2020**, *11*, 186 – 194.
[19] E. M. Hetrick, M. H. Schoenfisch, *Annu. Rev. Anal. Chem.* **2009**, *2*, 409 – 433.
[20] a) S. N. Sanders, M. K. Gangishetty, M. Y. Sfeir, D. N. Congreve, *J. Am. Chem. Soc.* **2019**, *141*, 9180 – 9184; b) Q. Liu, B. R. Yin, T. S. Yang, Y. C. Yang, Z. Shen, P. Yao, F. Y. Li, *J. Am. Chem. Soc.* **2013**, *135*, 5029 – 5037; c) F. Saenz, A. Ronchi, M. Mauri, R. Vadrucci, F. Meinardi, A. Monguzzi, C. Weder, *Adv. Funct. Mater.* **2021**, *31*, 2004495; d) P. Bharmoria, S. Hisamitsu, H. Nagatomi, T. Ogawa, M. A. Morikawa, N. Yanai, N. Kimizuka, *J. Am. Chem. Soc.* **2018**, *140*, 10848 – 10855.
[21] a) W. P. Wang, Q. Liu, C. Y. Zhan, A. Barhoumi, T. S. Yang, R. G. Wylie, P. A. Armstrong, D. S. Kohane, *Nano Lett.* **2015**, *15*, 6332 – 6338; b) L. Huang, Y. Zhao, H. Zhang, K. Huang, J. Y. Yang, G. Han, *Angew. Chem. Int. Ed.* **2017**, *56*, 14400 – 14404; *Angew. Chem.* **2017**, *129*, 14592 – 14596.
[22] Y. Zhao, Q. Q. Guo, X. M. Dai, X. S. Wei, Y. J. Yu, X. L. Chen, C. X. Li, Z. Q. Cao, X. E. Zhang, *Adv. Mater.* **2019**, *31*, 1806024.
[23] S. H. C. Askes, W. Pomp, S. L. Hopkins, A. Kros, S. Wu, T. Schmidt, S. Bonnet, *Small* **2016**, *12*, 5579 – 5590.
[24] N. Barraud, D. J. Hassett, S. H. Hwang, S. A. Rice, S. Kjelleberg, J. S. Webb, *J. Bacteriol.* **2006**, *188*, 7344 – 7353.
[25] N. S. Bryan, M. B. Grisham, *Free Radical Biol. Med.* **2007**, *43*, 645 – 657.
[26] a) D. F. Hu, L. Y. Zou, W. J. Yu, F. Jia, H. J. Han, K. Yao, Q. Jin, J. Ji, *Adv. Sci.* **2020**, *7*, 2000398; b) L. Hall-Stoodley, J. W. Costerton, P. Stoodley, *Nat. Rev. Microbiol.* **2004**, *2*, 95 – 108.
[27] a) R. Namivandi-Zangeneh, Z. Sadrearhami, A. Bagheri, M. Sauvage-Nguyen, K. K. K. Ho, N. Kumar, E. H. H. Wong, C. Boyer, *ACS Macro Lett.* **2018**, *7*, 592 – 597; b) E. M. Hetrick, J. H. Shin, N. A. Stasko, C. B. Johnson, D. A. Wespe, E. Holmuhamedov, M. H. Schoenfisch, *ACS Nano* **2008**, *2*, 235 – 246.
[28] S. C. Mansour, D. Pletzer, C. de la Fuente-Nunez, P. Kim, G. Y. C. Cheung, H. S. Joo, M. Otto, R. E. W. Hancock, *Ebiomedicine* **2016**, *12*, 219 – 226.
[29] a) G. Han, L. R. Martinez, M. R. Mihu, A. J. Friedman, J. M. Friedman, J. D. Nosanchuk, *PloS One* **2009**, *4*, e7804; b) D. Schairer, L. R. Martinez, K. Blecher, J. Chouake, P. Nacharaju, P. Gialanella, J. M. Friedman, J. D. Nosanchuk, A. Friedman, *Virulence* **2012**, *3*, 62 – 67.
[30] H. Zheng, G. O. Shang, S. Y. Yang, X. Gao, J. G. Xu, *Org. Lett.* **2008**, *10*, 2357 – 2360.
[31] M. J. Malone-Povolny, S. E. Maloney, M. H. Schoenfisch, *Adv. Healthcare Mater.* **2019**, *8*, 1801210.
[32] a) S. H. C. Askes, A. Bahreman, S. Bonnet, *Angew. Chem. Int. Ed.* **2014**, *53*, 1029 – 1033; *Angew. Chem.* **2014**, *126*, 1047 – 1051; b) A. Tokunaga, L. M. Uriarte, K. Mutoh, E. Fron, J. Hofkens, M. Sliwa, J. Abe, *J. Am. Chem. Soc.* **2019**, *141*, 17744 – 17753; c) J. Zhou, Q. Liu, W. Feng, Y. Sun, F. Y. Li, *Chem. Rev.* **2015**, *115*, 395 – 465; d) L. Huang, L. Zeng, Y. Z. Chen, N. Yu, L. Wang, K. Huang, Y. Zhao, G. Han, *Nat. Commun.* **2021**, *12*, 122.
[33] R. A. Marcus, *Angew. Chem. Int. Ed. Engl.* **1993**, *32*, 1111 – 1121; *Angew. Chem.* **1993**, *105*, 1161 – 1172.
[34] a) B. D. Ravetz, A. B. Pun, E. M. Churchill, D. N. Congreve, T. Rovis, L. M. Campos, *Nature* **2019**, *565*, 343 – 346; b) C. K. Prier, D. A. Rankic, D. W. C. MacMillan, *Chem. Rev.* **2013**, *113*, 5322 – 5363; c) N. A. Romero, D. A. Nicewicz, *Chem. Rev.* **2016**, *116*, 10075 – 10166.
[35] a) J. C. Theriot, C. H. Lim, H. Yang, M. D. Ryan, C. B. Musgrave, G. M. Miyake, *Science* **2016**, *352*, 1082 – 1086; b) J. T. Xu, K. Jung, A. Atme, S. Shanmugam, C. Boyer, *J. Am. Chem. Soc.* **2014**, *136*, 5508 – 5519; c) N. J. Treat, H. Sprafke, J. W. Kramer, P. G. Clark, B. E. Barton, J. Read de Alaniz, B. P. Fors, C. J. Hawker, *J. Am. Chem. Soc.* **2014**, *136*, 16096 – 16101.

Manuscript received: May 28, 2021
Revised manuscript received: June 22, 2021
Accepted manuscript online: July 1, 2021
Version of record online: ■■ ■■, ■■■■

Research Articles

Photoredox Catalysis

Z. Shen, S. Zheng, S. Xiao,* R. Shen, S. Liu,* J. Hu* ——— ■■■■–■■■■

Red-Light-Mediated Photoredox Catalysis Enables Self-Reporting Nitric Oxide Release for Efficient Antibacterial Treatment

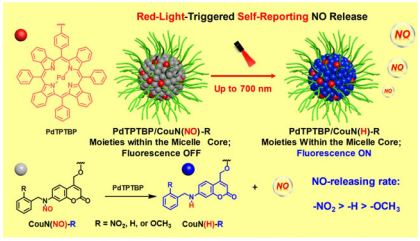

Red-light-mediated photoredox catalysis for self-reporting nitric oxide release is reported in the presence of palladium(II) tetraphenyltetrabenzoporphyrin. The NO-releasing platform eradicates *Pseudomonas aeruginosa* biofilm in vitro and treats bacterial infection in vivo.